

The Evolution of the Conductivity and Cathodoluminescence of the Films of Hafnium Oxide in the Case of a Change in the Concentration of Oxygen Vacancies

D. R. Islamov^{a, b}, V. A. Gritsenko^{a, b, c}, V. N. Kruchinin^a, E. V. Ivanova^{d, *},
M. V. Zamoryanskaya^d, and M. S. Lebedev^e

^a *Rzhanov Institute of Semiconductor Physics, Novosibirsk, 630090 Russia*

^b *Novosibirsk State University, Novosibirsk, 630090 Russia*

^c *Novosibirsk State Technical University, Novosibirsk, 630087 Russia*

^d *Ioffe Physical–Technical Institute, St. Petersburg, 194021 Russia*

^e *Nikolaev Institute of Inorganic Chemistry, Novosibirsk, 630090 Russia*

**e-mail: Ivanova@mail.ioffe.ru*

Received April 23, 2018

Abstract—The dependence of the conductivity of the films of hafnium oxide HfO_2 synthesized in different modes is studied. Depending on the modes of synthesis, the conductivity of HfO_2 at a fixed electric field of 1.0 MV/cm changes by four orders of magnitude. It is found that the conductivity of HfO_2 is limited by the model of phonon-assisted tunneling between the traps. The thermal and optical energies of the traps $W_1 = 1.25$ and $W_{\text{opt}} = 2.5$ eV, respectively, in HfO_2 are determined. It is found that the exponentially strong scattering of the conductivity of HfO_2 is due to the change in the trap density in a range of 4×10^{19} – 2.5×10^{22} cm^{-3} . In the cathodoluminescence spectra of HfO_2 , a blue band with the energy of 2.7 eV is observed which is due to the oxygen vacancies. A correlation between the trap density and intensity of cathodoluminescence, as well as between the trap density and refractive index, is found. A nondestructive in situ method for the determination of the trap density of hafnium oxide with the use of the measurement of the refractive index is proposed. The optimum values of the concentrations of oxygen vacancies for emitting devices on the basis of the films of HfO_2 are found.

DOI: 10.1134/S1063783418100098

INTRODUCTION

For over five decades, silica SiO_2 has been used as the key dielectric in silicon-based instruments. Currently, silica is replaced by dielectrics with a high dielectric permeability (high- κ) [1, 2]. Hafnium oxide HfO_2 is one of the most promising high- κ dielectrics for microelectronics. Hafnium oxynitrides and silicides are used as the gate dielectric in MOSFET and FinFET state-of-the-art transistors [3]. Currently, hafnium oxide is being intensively studied instead of silicon nitride as an active medium in flash memory devices [4] as well as in nonvolatile elements of resistive random access memory (RRAM) [5]. Resistive random access memory is fast (~ 0.1 – 10 ns) (for comparison, the time for reprogramming of a common flash memory card is 1 ms), consumes little energy (6 fJ/bit upon switching), has a high number of reprogramming cycles (no less than 10^{12}) in comparison with 10^4 cycles for common flash memory, stores information for ten years at 85°C , and is radiation-

resistant. A resistive memory element is a metal–dielectric–metal structure. The resistive memory effect consists in the reversible breakdown of the dielectric layer after applying a short voltage pulse; i.e., the state of the dielectric is translated from the high-resistance state to the low-resistance state (or vice versa). The translation of the state of a resistive memory element to the low-resistance state occurs due to the formation of a conductive metallic wire (filament) with a diameter of 1–10 nm that connects two conductive contacts [6]. The conductive filament is formed due to the diffusion of oxygen vacancies (V_{O}) in strong electric and temperature fields. The physics of the switching of a resistive memory element that is determined by the dynamics of the oxygen vacancies is still unclear and is the subject of a large body of research [7–9]. Two promising applications of RRAM are proposed, namely, as nonvolatile memory matrices and for neuromorphic applications [5].

The mechanism of charge transport in HfO_2 was a subject of active research [10, 11]. It was found that the conductivity of HfO_2 in a strong electric field is limited by phonon-assisted tunneling between the traps which was considered for the first time by Nasyrov and Gritsenko (N–G) [12, 13]

$$P = \int_{\varepsilon < 0} \frac{\hbar |\varepsilon|}{m^* s^2 k T Q_0} \exp\left(-\frac{(Q - Q_0)^2 + (Q - qFs/Q_0)^2}{2kT}\right) - \frac{4\sqrt{2m^*}((- \varepsilon)^{3/2} - (-qFs - \varepsilon)^{3/2})}{3 qF\hbar} dQ, \quad (1)$$

$$\varepsilon = -Q_0(Q - Q_0) - W_{\text{opt}}, \quad Q_0 = \sqrt{2(W_{\text{opt}} - W_t)},$$

where P is the rate (probability per unit time) of tunneling between adjacent traps, ε is the energy of the electron localized on the phonon-bound trap, \hbar is the Plank constant, m^* is the effective mass, s is the average distance between the traps, k is the Boltzmann constant, T is the temperature, Q is the configuration coordinate, q is the elementary charge (in absolute magnitude), F is the electric field, W_t is the energy of thermal ionization of the trap, and W_{opt} is the energy of optical ionization of the trap. At

$$qFs \ll W_t, \quad (2)$$

expression (1) can be calculated by a saddle-point method, and, taking into account reverse transitions (against the field), obtains

$$P = \frac{2\sqrt{\pi}\hbar W_t}{m^* s^2 Q_0 \sqrt{kT}} \exp\left(-\frac{W_{\text{opt}} - W_t}{2kT}\right) \times \exp\left(-\frac{2s\sqrt{2m^*} W_t}{\hbar}\right) \sinh\left(\frac{qFs}{2kT}\right). \quad (3)$$

The rate of tunneling acquires clearer sense in this form. The preexponential factor corresponds to the rate factor. The first exponent is indicative of the activation mechanism of excitation with the energy $(W_{\text{opt}} - W_t)/2$, which should be overcome in the case of an act of tunneling from one trap to the adjacent trap. The second exponent is the factor of tunnel penetrability of the potential barrier. The third exponential factor, the decrease in the potential barrier in the electric field, is reduced to a hyperbolic sine when reverse transitions “against the field” are taken into account. The analytical dependence of the current density J on the electric field for the tunneling between traps was obtained in [14]

$$J = \frac{q}{s^2} \frac{n_t}{N} \left(1 - \frac{n_t}{N}\right) P, \quad (4)$$

where n_t is the filled trap density and N is the total trap density. On the approximation of uniform distribution of traps throughout the volume, the trap density and average distance between them are tied by the correlation $N = s^{-3}$, and s^2 has the sense of capture cross section per trap. It is seen from expression (4) that the

maximum current flows at $n_t/N = 0.5$. The analysis of the experimental data under the model of phonon-assisted tunneling makes it possible to determine the average distance between the traps, and, therefore, the trap density in the dielectric. It was recently found that oxygen vacancies (V_O) serve as the traps in HfO_2 [11, 15]. The electron transitions on V_O in HfO_2 are responsible for the blue luminescence band with the maximum at 2.7 eV [16, 17]. The aim of this work is to study the influence of the concentration of oxygen vacancies in hafnium oxide on the intensity of the blue luminescence band.

SAMPLES AND MEASUREMENTS

The optical and transport measurements were performed for the films of HfO_2 with a thickness of 40 nm synthesized on a Si(100) substrate via atomic layer deposition (ALD) with different systems of precursors. For the synthesis of the first series of samples, TEMAH (tetrakis(ethylmethanamide)hafnium(IV), $\text{Hf}(\text{NCH}_2\text{C}_2\text{H}_5)_4$) precursors in combination with water H_2O were used at the temperature of the substrate of 250°C [18–20]. The second series of samples was synthesized using a system of precursors new for the ALD technology, namely, $\text{Hf}(\text{thd})_4$ (2,2,6,6-tetramethylheptane-3,5-dionate hafnium(IV)) with molecular oxygen O_2 as the oxidizing agent at the temperature of the substrate of 440°C. Both series of samples were annealed directly in the reactor in a flow of N_2 for 1 h at different temperatures. The temperatures of annealing were $T_{\text{ann}} = 550$ and 700°C for the $\text{Hf}(\text{thd})_4\text{--O}_2$ series (samples *b* and *c*) and $T_{\text{ann}} = 440$, 550, and 700°C for the TEMAH– H_2O series (samples *f*, *e*, and *g*). After annealing, the samples were slowly cooled down in the reactor to room temperature. Samples *a* ($\text{Hf}(\text{thd})_4\text{--O}_2$) and *d* (TEMAH– H_2O) were not subjected to the additional annealing procedure, and T_{ann} for them corresponded to the temperature of the synthesis. The films of HfO_2 synthesized by both methods are polycrystalline with the crystallites of the monoclinic phase.

The thicknesses and optical properties of the films before and after annealing were controlled via the methods of spectral ellipsometry. The procedure for ellipsometric measurements was similar to the procedure described in [21]. For the convenience of comparison and analysis of the results of the measurements, the refractive index and thickness of the films are presented in this work at a wavelength of a helium–neon laser $\lambda = 632.8$ nm ($h\nu = 1.96$ eV).

For transport measurements, metal–oxide–semiconductor (MOS) structures were formed. For this, Al electrodes with an area of 0.5 mm² were sprayed onto the films of HfO_2 through a metallic mask. The voltage–current characteristics (VCC) of the test MOS structures were measured using a Keithley 4200-SCS

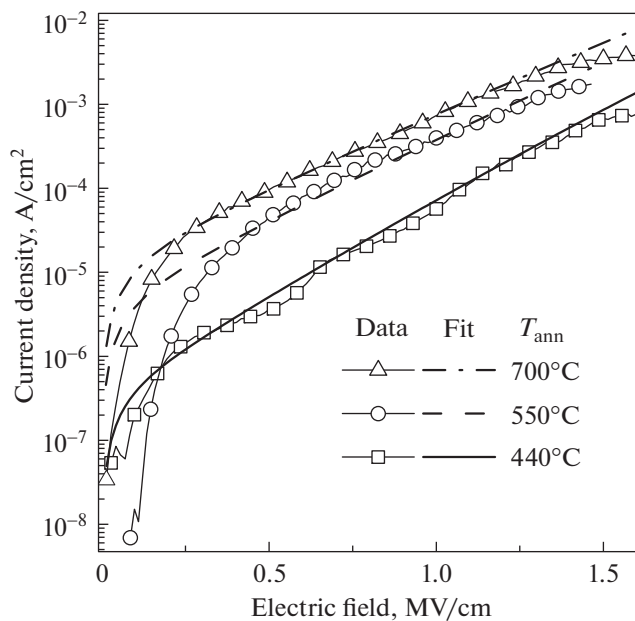


Fig. 1. Experimental (symbols) and calculated (lines) voltage–current characteristics of the n -Si/HfO₂/Al structure from the Hf(thd)₄–O₂ series.

parametric analyzer in a quasi-stationary mode at room temperature.

The cathodoluminescence spectra for the films of HfO₂ were obtained on a CAMEBAX electron probe microanalyzer (CAMECA) equipped with an optical spectrometer with an original design [22]. The measurements were performed at the electron beam current of 30 nA, diameter of the electron beam of ~ 10 μ m, and energy of electrons of 5 keV.

THE CONDUCTIVITY OF HfO₂ SYNTHESIZED IN DIFFERENT MODES

In Fig. 1, the symbols represent the experimental VCC for MOS structures a , b , and c from the Hf(thd)₄–O₂ series. It is seen that the current exponentially depends on the electric field in the dielectric and temperature of annealing. Increasing T_{ann} leads to an increase in the leakage currents and an insignificant decrease in the inclination on a semilogarithmic scale. The analysis under the N–G theory made it possible to describe the experimental data at the thermal and optical energies of the traps $W_t = 1.25$ and $W_{\text{opt}} = 2.5$ eV, respectively, which correspond to the oxygen vacancies V_O in HfO₂ [10, 11]. In the case of annealing, the trap density increases to the value of 9×10^{19} cm⁻³. The numerical analysis showed that, in high fields $F > 1$ MV/cm, condition (2) was not fulfilled, and VCC calculated by (3) and (4) significantly diverged with the dependences calculated from (1) and (4). Because of this, hereinafter, model VCC were calcu-

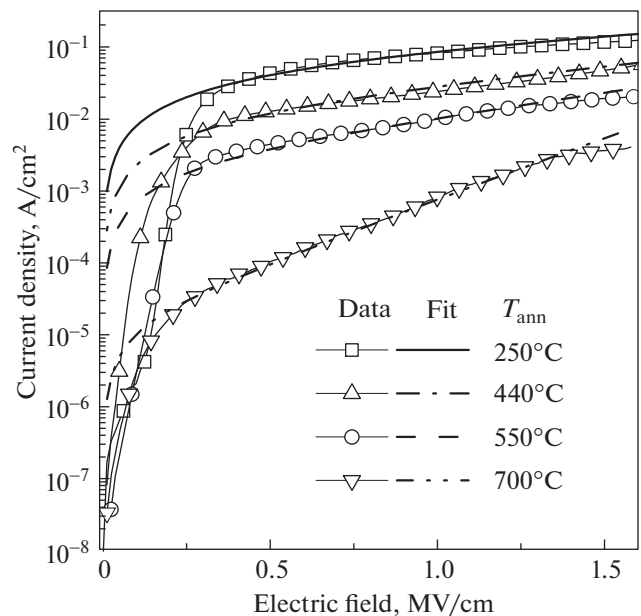


Fig. 2. Experimental (symbols) and calculated (lines) voltage–current characteristics of the n -Si/HfO₂/Al structure from the TEMAH–H₂O series.

lated using expressions (1) and (4). Lines in Fig. 1 show the results of the modeling under the N–G theory.

In Fig. 2, symbols represent the experimental VCC for MOS structures d , e , f , and g from the TEMAH–H₂O series. The current exponentially depends on the electric field in the dielectric and temperature of annealing. Increasing T_{ann} leads to a decrease in the leakage currents and a growth in the inclination on a semilogarithmic scale. The analysis under the N–G theory made it possible to describe the experimental data at the thermal and optical energies of the traps $W_t = 1.25$ and $W_{\text{opt}} = 2.5$ eV, respectively (lines in Fig. 2). In the case of annealing, the trap density decreases to the value of 9×10^{19} cm⁻³.

THE DEPENDENCE OF THE TRAP DENSITY ON THE SYNTHESIS METHOD AND TEMPERATURE OF ANNEALING

Figure 3 presents the dependences of the calculated in the previous chapter trap densities for the films of HfO₂ synthesized under different conditions on the temperature of annealing.

In the films of HfO₂ synthesized in the Hf(thd)₄–O₂ system, the increase in the temperature of annealing in nitrogen from 440 to 700°C leads to an insignificant increase in the trap density from 2×10^{19} to 9×10^{19} cm⁻³. In HfO₂ synthesized in the TEMAH–H₂O system, the increase in the temperature of annealing in nitrogen from 250 to 700°C leads to a significant

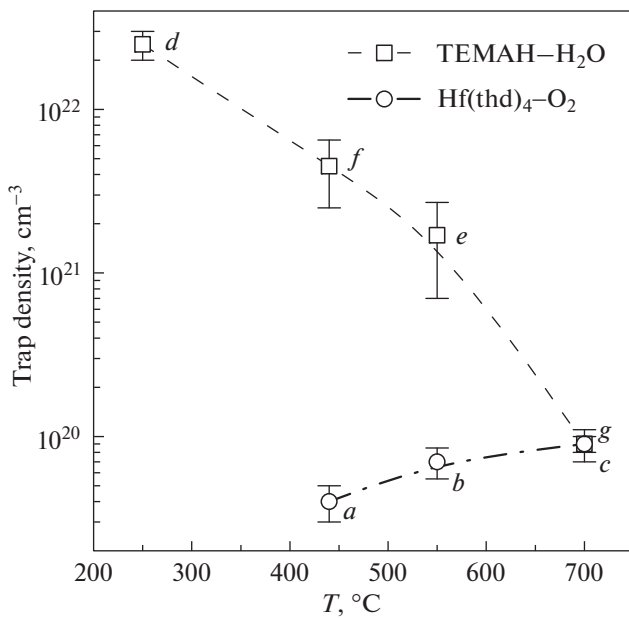
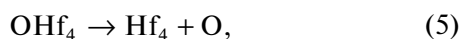


Fig. 3. The dependence of the electron trap density on the synthesis conditions of the films of HfO_2 .

decrease in the trap density from 2.5×10^{22} to $9 \times 10^{19} \text{ cm}^{-3}$.

It was found by us earlier that oxygen vacancies serve as the traps in HfO_2 [10, 11, 17]. Because of this, the trap density in Fig. 3 is equal to the concentration of oxygen vacancies and, therefore, our task is to explain the evolution of the concentration of oxygen vacancies of HfO_2 synthesized via two methods in the case of annealing in nitrogen. We explain the different behavior of the trap density in the case of annealing depending on the synthesis method of HfO_2 by the presence or absence of hydroxyl groups OH in the oxygen-containing reagents.

Start with a simple case—an increase in the concentration of oxygen vacancies in the case of annealing of HfO_2 synthesized in the $\text{Hf}(\text{thd})_4\text{-O}_2$ system. In the $\text{Hf}(\text{thd})_4\text{-O}_2$ system, OH groups are absent in the molecules of precursors, and their formation is unsubstantial in the ALD process. In the monoclinic phase of HfO_2 , hafnium atoms are coordinated by seven oxygen atoms, and it consists of HfO_7 structural units. A half of the oxygen atoms in these phases is coordinated by four Hf atoms (a OHf_4 structural unit), and the second half of oxygen atoms is coordinated by three Hf atoms (a OHf_3 structural unit). Annealing in an inert atmosphere leads to the breaking of the Hf–O bonds according to the following reactions and formation of clusters from hafnium atoms: for a fourfold coordinated oxygen atom (a fourfold coordinated vacancy)

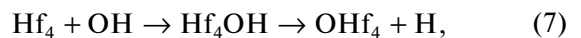


and for a threefold coordinated oxygen atom (a threefold coordinated vacancy)

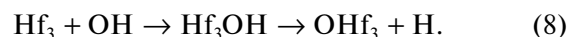


Symbols Hf_4 and Hf_3 in (5) and (6) denote the fourfold and threefold coordinated oxygen vacancies in the monoclinic phase of HfO_2 , respectively. Therefore, in HfO_2 synthesized in the $\text{Hf}(\text{thd})_4\text{-O}_2$ system, the increase in the trap density in the case of annealing in nitrogen is explained by the formation of oxygen vacancies.

In the films of HfO_2 from the TEMAH– H_2O series, the explanation of the evolution of the trap density in the case of annealing in nitrogen is associated with the presence of hydroxyl groups OH. The presence of OH groups in the TEMAH– H_2O films of HfO_2 was confirmed by IR spectroscopy; here, a sharp decrease in their concentration in the case of annealing in a nitrogen atmosphere at 700°C was recorded [23]. Since hydroxyl groups are an indispensable attribute of ALD processes on the basis of H_2O , a certain number of hydroxyl groups OH which did not react with TEMAH is embedded into the structure of the film. Increasing the temperature of annealing of the TEMAH– H_2O films of HfO_2 leads to a decrease in the concentration of oxygen vacancies from 2.5×10^{22} to $9 \times 10^{19} \text{ cm}^{-3}$. This phenomenon is explained by the annihilation of oxygen vacancies in the case of their interaction with the hydroxyl groups present in the film according to the following reactions: a fourfold coordinated vacancy



and for a threefold coordinated vacancy



Therefore, the decrease in the trap density in HfO_2 synthesized in the TEMAH– H_2O system in the case of annealing in nitrogen is explained by the annihilation of oxygen vacancies due to the chemical interaction with hydroxyl groups. Here, the “terminal” OH groups first become “bridge” in the case of migration of the complex to the place of the oxygen vacancy with the saturation of the Hf–O bonds, after which the hydroxyl group falls apart followed by the removal of the hydrogen atom.

THE CORRELATION OF THE TRAP DENSITY AND REFRACTIVE INDEX OF HfO_2

Figure 4 presents the dependence of the refractive index of HfO_2 on the trap density. With the growth in the trap density, the refractive index of HfO_2 increases. It is an expected effect. Since oxygen vacancies serve as the traps in hafnium oxide, the enrichment of hafnium oxide with the metal is accompanied by an increase in the refractive index. The refractive index of metallic hafnium at a wavelength of a helium–neon

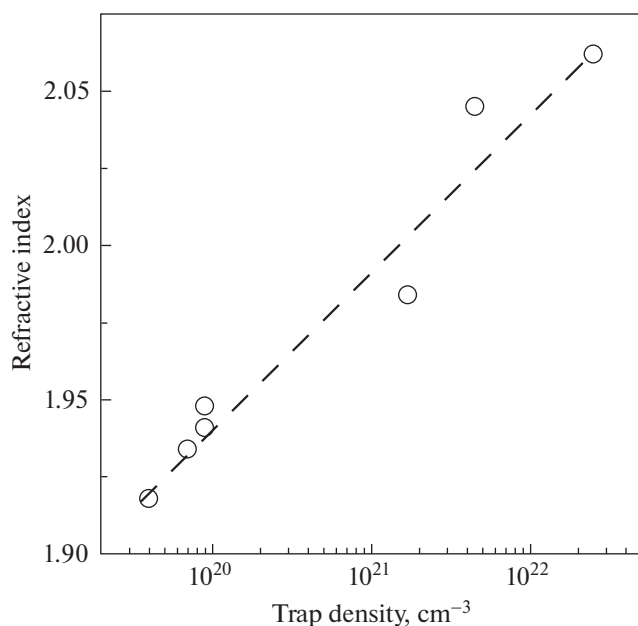


Fig. 4. The dependence of the refractive index of HfO_2 measured at a wavelength of a helium–neon laser on the trap density.

laser is equal to the value $n = 2.766$. Because of this, the enrichment with the metal is accompanied by an increase in the refractive index. The dependence of the refractive index of HfO_2 on the trap density in Fig. 4 opens up the possibility for the nondestructive method for the determination of the trap density during the synthesis.

CATHODOLUMINESCENCE OF THE FILMS OF HfO_2 WITH DIFFERENT TRAP DENSITIES

Cathodoluminescence (CL) spectra were obtained for the films of HfO_2 (Fig. 5). The measurements of the CL in several random regions for each sample showed that the films of HfO_2 were quite uniform in the lateral direction. A wide band with the maximum at 2.75 eV is observed for samples *a* and *b* synthesized in the $\text{Hf}(\text{thd})_4\text{--O}_2$ system, and a band with the maximum at 2.0 eV are also observed in sample *c*. Two emission maxima at 2.0 and 2.6 eV can be distinguished in the CL spectra of the samples synthesized in the $\text{TEMAH--H}_2\text{O}$ system. The CL spectra were approximated by a sum of two Gauss curves. As a result of the approximation, the following spectral characteristics of the bands were obtained for the samples synthesized in the $\text{Hf}(\text{thd})_4\text{--O}_2$ system: 2.75 ± 0.01 eV (FWHM = 0.87 ± 0.01 eV) and 1.97 ± 0.02 eV (FWHM = 0.45 ± 0.01 eV); and for the films synthesized in the $\text{TEMAH--H}_2\text{O}$ system: 2.60 ± 0.02 eV (FWHM = 0.45 ± 0.01 eV) and 1.98 ± 0.02 eV (FWHM = 0.45 ± 0.01 eV).

It was shown earlier that the presence of trapping levels near the luminescence centers can cause a change in the intensity of cathodoluminescence in the case of continuous irradiation of a sample by an electron beam [24, 25]. In this connection, the studies of the change in the intensity of the CL bands under the action of an electron beam were performed in order to study the influence of the traps on the emissive centers in the films of HfO_2 . The change in the intensity of the cathodoluminescence band under the action of an electron beam was studied as follows: the wavelength, at which the dynamics of the change in the intensity of CL was measured, was selected in such a way as to minimize the influence of the adjacent emission bands (Fig. 6). In the blue range, the dynamics was studied at the energies of photons of 2.6 and 3.3 eV. This is associated with the fact that, in the samples synthesized in the $\text{Hf}(\text{thd})_4\text{--O}_2$ system, the maximum of luminescence in the blue range is shifted from 2.6 to 2.75 eV, and the half-width is increased twofold, which can be interpreted as either the occurrence of an additional band with the maximum of 3.3 eV or as the changes in the properties of the luminescence center. The dynamics of the intensity of CL for different wavelengths is presented in Fig. 7. As is seen, an increase in the intensity of CL in the blue range of 2.6–3.3 eV is observed in both samples, and no changes in the intensity in the red range are observed.

The most probable reason for the increase in the intensity of the cathodoluminescence bands in the films of HfO_2 in the process of irradiation by an electron beam is traps which are located near the energy level responsible for the luminescence in the corresponding range [24]. The following model of the interaction of the trapping and emissive levels can be proposed [25]. In this model, the traps do not directly participate in the radiative recombination; however, they can serve as an additional channel for the nonradiative recombination from the energy level responsible for the luminescence. Thus, with the filling of the trapping levels, the number of free traps capable of capturing the excitation from the emissive level drops, and the carrying capacity of this channel of nonradiative recombination becomes smaller. Due to the finite number of trapping levels, the intensity of luminescence from the level under consideration increases with time reaching the saturation at the moment when all the traps turn out to be filled. In this case, the time of the increase in the intensity depends on the excitation density and probability of the capture of an electron by a trap [25].

On the grounds that the time of the increase in the intensity of CL under the action of an electron beam turned out to be the same for the radiant energies of 2.6 and 3.3 eV, a conclusion was drawn that this emission was associated with one emission transition of the luminescence center. Because the buildup time of CL depends only on the excitation density and probability

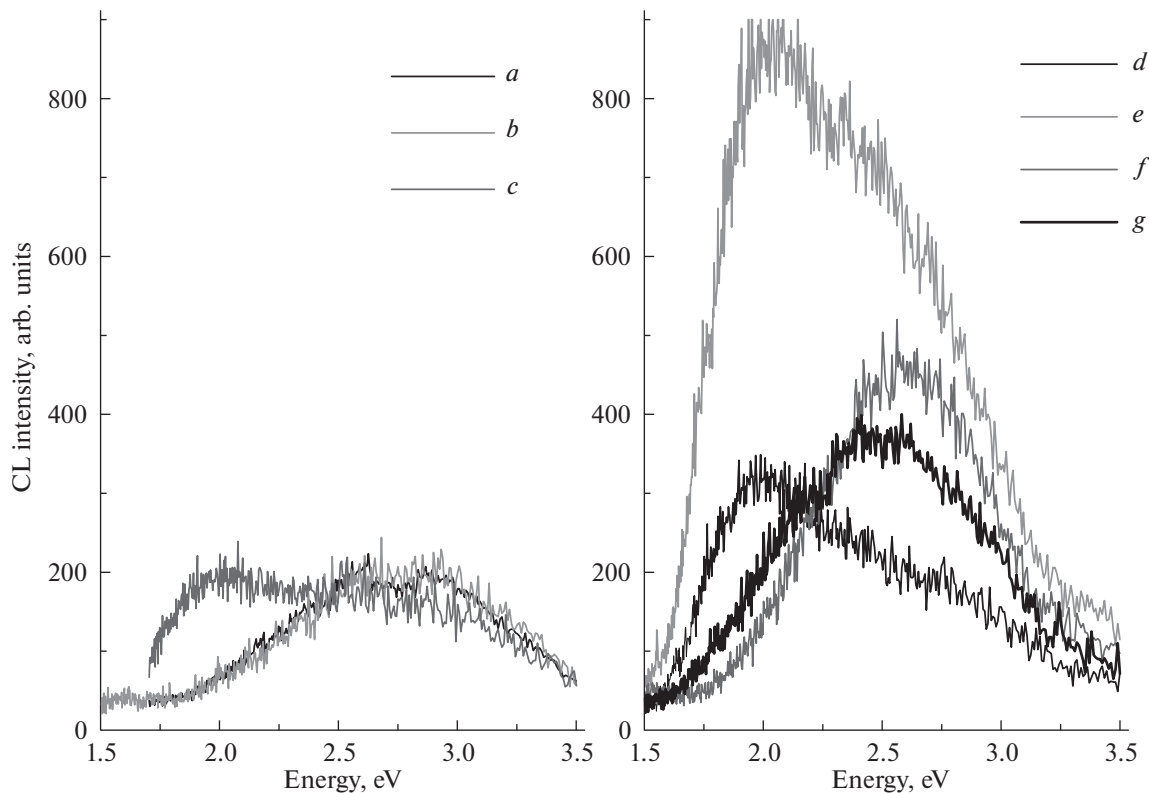


Fig. 5. CL spectra of different samples of HfO_2 .

of the capture of an electron by a trap, it can be suggested that the probabilities of the capture of an electron in samples *c* and *d* synthesized in different systems are the same, which also confirms the assumption about the similar nature of the traps. In this connection, it can be assumed that, for the samples

grown using different methods, the radiant energy of the luminescence centers shifts from 2.6 to 2.75 eV. The different position of the emission maximum in the blue range can be associated with the different concentration of OH groups in the synthesized films.

The drawn conclusions about the fact that the band in the blue range is associated with one type of luminescence centers made it possible to construct a dependence of the intensity of CL in the blue range for the samples with different trap densities (Fig. 8).

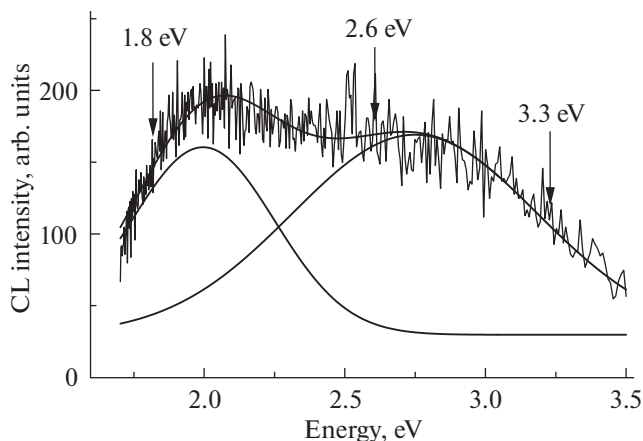


Fig. 6. The CL spectrum of film *c* and approximation by a sum of two Gauss curves. The arrows indicate the spectral regions, in which the dynamics of the intensity of CL were obtained under the prolonged irradiation by an electron beam.

RESULTS AND DISCUSSION

The Nasyrov–Gritsenko (N–G) model of phonon-assisted tunneling quantitatively explains the exponentially strong scattering of the value of the leakage current of HfO_2 depending on the modes of synthesis of the films. Changing the value of the current in the N–G model is explained by the exponentially strong dependence of the probability of phonon-assisted tunneling on the distance s between the traps, and, hence, trap density $N = s^{-1/3}$. The N–G model makes it possible to determine the trap density in HfO_2 synthesized in different modes by the slope of the $\log(J)–F$ dependence.

The decrease in the leakage current of HfO_2 synthesized in the TEMAH– H_2O system by five orders of

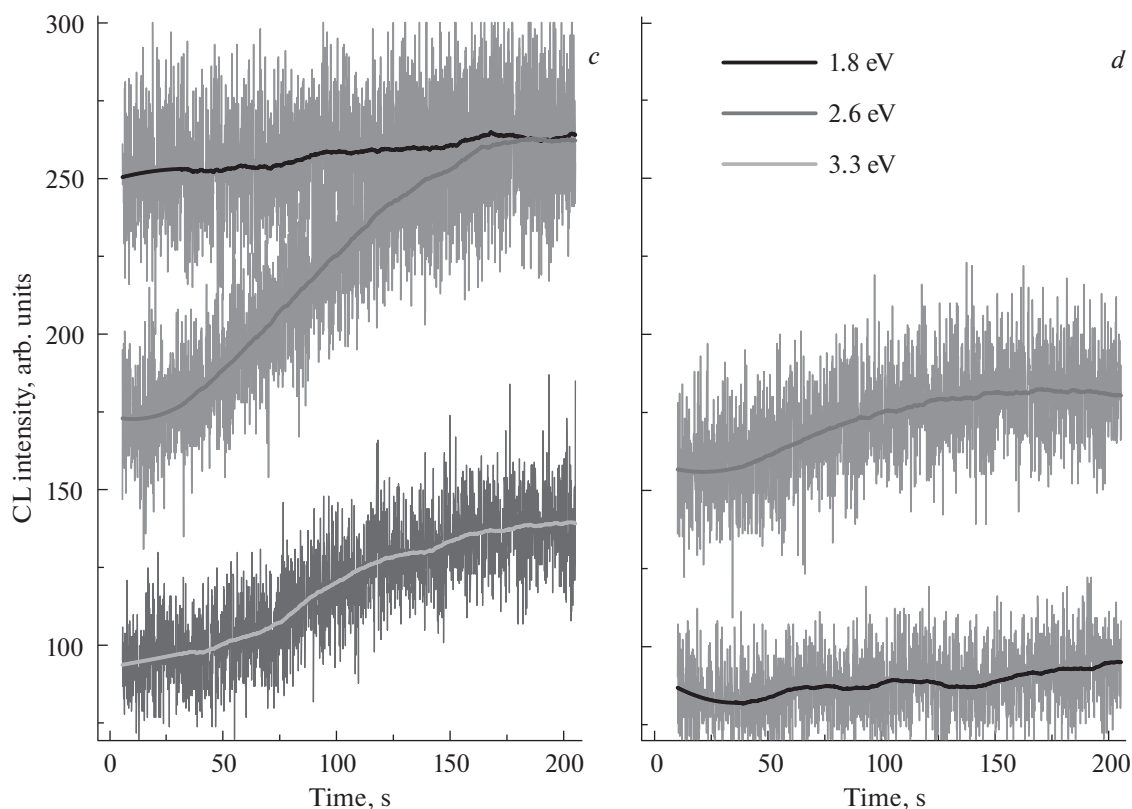


Fig. 7. The dynamics of the intensity of the CL bands for samples *c* and *d* for different wavelengths under constant irradiation by an electron beam.

magnitude is explained by the decrease in the concentration of oxygen vacancies due to the interaction with hydroxyl groups. The increase in the leakage current of

HfO₂ synthesized in the Hf(thd)₄–O₂ system is determined by the formation of oxygen vacancies due to the breaking of the Hf–O bonds.

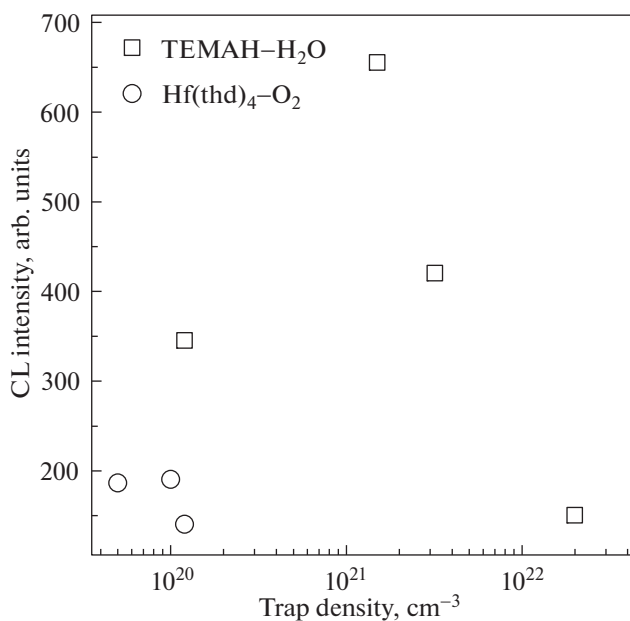


Fig. 8. The intensity of the band in the blue range for different samples depending on the trap density.

The refractive index of hafnium oxide logarithmically increases with the growth in the trap density, concentration of oxygen vacancies. This is due to the enrichment of hafnium oxide with the excessive metal. The found correlation between the refractive index and trap density opens up the possibility for the use of a nondestructive in situ quality control method (the estimation of the trap density, concentration of oxygen vacancies) of the films of metal oxides including HfO₂ during the synthesis.

Since the growth in the intensity is observed only for the band in the blue range, it can be assumed that the traps do not interact with the luminescence centers that give luminescence, with a maximum of 2.0 eV.

During the analysis of the experimental data for the purpose of finding the correlation between the trap density and intensity of luminescence, two limiting alternative options were expected, namely, either an increase in the intensity of cathodoluminescence with the increase in the trap density or a decrease in the intensity of cathodoluminescence with the increase in the trap density due to the effect of concentration quenching [16]. As a result of experimental measurements, a nonmonotone dependence between the trap

density in HfO_2 and intensity of luminescence was found. Three main sections can be distinguished in the intensity-versus-concentration of defects dependence (Figs. 6 and 7). At the concentrations of defects of less than 10^{20} cm^{-3} , a decrease in the intensity of the blue cathodoluminescence band with the depletion of the film of oxygen is observed. Then the intensity of luminescence starts increasing and, after reaching the maximum at $N \sim 10^{21} \text{ cm}^{-3}$, the growth changes to a drop.

The section of the dependence which corresponds to the increase in the intensity of luminescence with the depletion of hafnium oxide of oxygen can be explained by the increase in the number of optically active centers. Further decrease can be explained by the effect of concentration quenching. The decrease in the intensity of CL in the case of irradiation of HfO_2 by an electron beam is also indicative of the concentration quenching of luminescence [26]. Therefore, the following optimum range of oxygen vacancies in HfO_2 that act as the optically active centers for emitting devices on the basis of hafnium oxide can be distinguished: $3-10 \times 10^{20} \text{ cm}^{-3}$.

CONCLUSIONS

In this work, the dependence of the leakage currents of HfO_2 depending on the modes of synthesis was studied. The exponentially strong change in the conductivity depending on the modes of synthesis is explained by the Nasyrov–Gritsenko model of phonon-assisted tunneling of electrons between adjacent traps. An explanation for the evolution of the trap density of the films of HfO_2 synthesized via two methods in the case of annealing in nitrogen was proposed. The correlation between the trap density and intensity of cathodoluminescence of HfO_2 was found. A new non-destructive in situ method for the determination of the trap density of hafnium oxide with the use of the measurement of the refractive index was proposed. The optimum range of concentrations of oxygen vacancies for emitting devices on the basis of the films of HfO_2 was found.

ACKNOWLEDGMENTS

This work was partially financially supported by the Russian Science Foundation, grant no. 16-19-00002.

REFERENCES

1. J. Robertson, Rep. Prog. Phys. **69**, 327 (2006).
2. T. V. Perevalov and V. A. Gritsenko, Phys. Usp. **53**, 561 (2010).
3. T. Ando, U. Kwon, S. Krishnan, M. M. Frank, and V. Narayan, in *Thin Films on Silicon, Electronic and Photonic Applications*, Ed. by V. Narayanan, M. M. Frank, and A. Demkov (World Scientific, Singapore, 2016), p. 323.
4. H. Zhu, J. E. Bonevich, H. Li, C. A. Richter, H. Yuan, O. Kirillov, and Q. Li, Appl. Phys. Lett. **104**, 233504 (2014).
5. V. A. Gritsenko and D. R. Islamov, *Physics of Dielectric Films: Mechanisms of Charge Transport and Physical Principles of Memory Devices* (Parallel', Novosibirsk, 2017) [in Russian].
6. G. Bersuker, D. C. Gilmer, D. Veksler, P. Kirsch, L. Vandelli, A. Padovani, L. Larcher, K. McKenna, A. Shluger, V. Iglesias, M. Porti, and M. Nafria, J. Appl. Phys. **110**, 24518 (2011).
7. S. Balatti, S. Larentis, D. C. Gilmer, and D. Ielmini, Adv. Mater. **25**, 1474 (2013).
8. A. A. Chernov, D. R. Islamov, A. A. Pik'nik, T. V. Perevalov, and V. A. Gritsenko, ECS Trans. **75**, 95 (2017).
9. T. V. Perevalov and D. R. Islamov, ECS Trans. **80**, 357 (2017).
10. D. R. Islamov, V. A. Gritsenko, C. H. Cheng, and A. Chin, Appl. Phys. Lett. **105**, 222901 (2014).
11. V. A. Gritsenko, T. V. Perevalov, and D. R. Islamov, Phys Rep. **613**, 1 (2016).
12. K. A. Nasyrov and V. A. Gritsenko, J. Exp. Theor. Phys. **112**, 1026 (2011).
13. K. A. Nasyrov and V. A. Gritsenko, Phys. Usp. **56**, 999 (2013).
14. D. R. Islamov, V. A. Gritsenko, and A. Chin, Optoelectron., Instrum. Data Process. **53**, 184 (2017).
15. T. V. Perevalov, V. Sh. Aliev, V. A. Gritsenko, A. A. Sarraev, V. V. Kaichev, E. V. Ivanova, and M. V. Zamoryanskaya, Appl. Phys. Lett. **104**, 071904 (2014).
16. E. V. Ivanova, M. V. Zamoryanskaya, V. A. Pustovarov, V. Sh. Aliev, V. A. Gritsenko, and A. P. Yelissev, J. Exp. Theor. Phys. **120**, 710 (2015).
17. V. Gritsenko, D. Islamov, T. Perevalov, V. Aliev, A. Yelissev, E. Lomanova, V. Pustovarov, and A. Chin, J. Phys. Chem. C **120**, 19980 (2016).
18. K. Kukli, M. Ritala, T. Sajavaara, J. Keinonen, and M. Leskelä, Chem. Vapor Depos. **8**, 199 (2002).
19. C. Liu, Y. M. Zhang, Y. M. Zhang, and H. L. Lv, J. Appl. Phys. **116**, 222207 (2014).
20. J. Gope, Vandana, N. Batra, J. Panigrahi, R. Singh, K. K. Maurya, R. Srivastava, and P. K. Singh, Appl. Surf. Sci. **357**, 635 (2015).
21. V. A. Shvets, V. N. Kruchinin, and V. A. Gritsenko, Opt. Spectrosc. **123**, 728 (2017).
22. M. V. Zamoryanskaya, S. G. Konnikov, and A. N. Zamoryanskii, Instrum. Exp. Tech. **47**, 477 (2004).
23. M.-T. Ho, Y. Wang, R. T. Brewer, L. S. Wielunski, and Y. J. Chabal, Appl. Phys. Lett. **87**, 133103 (2005).
24. K. N. Orekhova, R. Tomala, D. Hreniak, W. Strek, and M. V. Zamoryanskaya, Opt. Mater. **74**, 170 (2017).
25. M. V. Zamoryanskaya and A. N. Trofimov, Opt. Spectrosc. **114**, 79 (2013).
26. A. N. Trofimov and M. V. Zamoryanskaya, J. Surf. Invest.: X-Ray, Synchrotr. Neutron Tech. **3**, 15 (2009).

Translated by E. Boltukhina